ISSN: 2641-2039
DOI: 10.33552/GJES.2021.07.000662
Global Journal of Engineering Sciences
Iris Publishers

Research Article



# Heat Transfer Characteristics of Submerged and Free Surface Air-assistant Water Jet Impingement

**Victoria J Rouse and Kyosung Choo***

*Mechanical Engineering, Youngstown State University, Youngstown, United States*

***Corresponding author:** Kyosung Choo, Mechanical Engineering, Youngstown State University, Youngstown, OH 44555, USA.

**Received Date:** March 13, 2021

**Published Date:** March 19, 2021

## Abstract

Heat transfer and fluid flow characteristics of air-assistant submerged and free surface water impinging jets are experimentally investigated. Results showed that the Nusselt number and pressure decrease exponentially in both free surface and submerged jets for all volumetric qualities in jet deflection region. In transition region, the Nusselt number and pressure of the submerged jet and free surface jet decrease since the jet deflection effect was disappeared. In buoyance effect region, the Nusselt number and pressure increase in the free surface jet since the potential energy increases, while the Nusselt number and pressure decrease in the submerged jet since the bubbles are not impinged the plate due to the buoyancy effect.

**Keywords:** Two-phase; Impinging jet; Heat transfer; Circular jet

## Introduction

Impinging jets have been studied in great depth due to their high rates of heat transfer and wide range of application [1-4]. Several researchers have observed heat transfer and fluid flow characteristics for single phase and two-phase free surface jet impingement. For the single-phase free surface jet impingement, Kuraan et al. [5] studied the nozzle-to-plate spacings effect on heat transfer and found correlations for hydraulic jump diameter and local Nusselt number. Friedrich et al. [6] investigated the effects of volumetric quality on thermal performance of two-phase impinging jets and showed the optimum design of the jet impingement.

In a submerged jet, the jet ejects into a fluid of the same state before impinging on a surface, where the entrainment of the surrounding fluid is significant. Choo et al. [7] experimentally investigated thermal characteristics on a flat plate and showed that the governing parameter of the heat transfer is stagnation pressure. Bieber et al. [8] numerically investigated the submerged laminar slot jet impingement. They suggested correlations for submerged slot jets as functions of nozzle-to-plate distance, heat flux, and wall temperature. The purpose of this study is to determine the heat transfer and fluid flow characteristics of two-phase submerged and free surface impinging jets and compare the two impinging jets.

## Material and Methods

Figure 1 shows a schematic diagram of the test section [9-12]. The water flow is regulated by a flowmeter valve (Dwyer® RMB-84-SSV). The range of the flowmeter valve is 0- 2.52 liter per minute. The air was also regulated by two mass flow controllers. The flow controller used depended on the volumetric quality of the mixture. For lower volumetric qualities (β = 0.1,0.3,0.5), the Omega® FMA5514A was used, which has a full-scale range of 0-1000 mL/min. For higher volumetric qualities (β = 0.7), the Omega® FMA5520A was used with an accuracy level of ±1% and a repeatability of ±0.15%, and a full-scale range of 0-10 L/min. To create the two-phase impinging jet, the two fluids are regulated in separate tubes and then combined in a single nozzle. The

volumetric quality was controlled by keeping the flow rate of the water constant at 1.47 x 10-5 m3/s throughout the experiment and varying the air flow rate in order to change the volumetric quality. The nozzle in which the fluids are combined is 470 mm long and is made of extruded acrylic. The nozzle has a diameter of 5.86 mm, and is circular, producing an axisymmetric velocity profile. The nozzle is mounted on a 3-axis stage (Thorlabs, Inc, PT3A/M) that has a resolution of 10 μm. Two digital manometers were used to measure the pressure at the stagnation zone of the impinging jet: Meriam® M200-DI0001 manometer with a range of 0 – 6.9 kPa and an accuracy of ±0.05% FS; and Meriam® M200-DI0005 manometer with range of 0 – 34.5 kPa and similar accuracy.

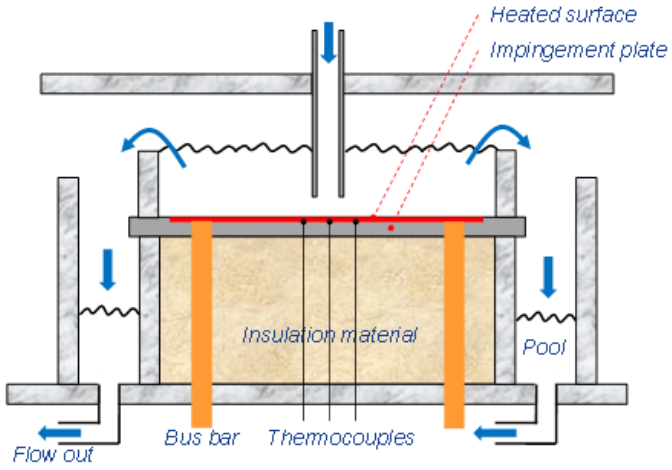


**Figure 1:** Test section configuration.

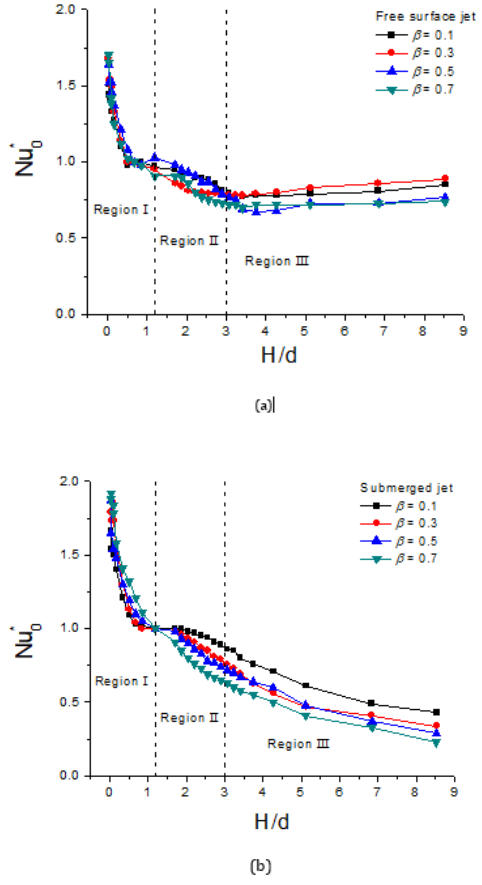


**Figure 2:** Normalized stagnation Nusselt number: (a) free surface jet (b) submerged jet.

The circular impingement surface is inside the test section, but elevated so that water can fall off of it and fall into the pool below. This is useful in the case of the free surface jet, because the water exiting the nozzle can flow off of the plate after it passes over the stagnation point without effecting the flow at the stagnation point. The focus of this study is to compare the free surface jet and the submerged jet. For the submerged portion, the jet is submerged in a cylindrical tank that is 141.7 mm in diameter and 43.2 mm in height as shown in Figure 2. The impingement surface was made of PTFE Teflon and is a disk that is 20 mm thick and 297 mm in diameter.

## Results and Discussion

The variation of the normalized Nusselt number, Nu0* (Nu0 / Nu0, H/d = 1) and the normalized pressure P0* (P0 / P0, H/d = 1) of each nozzle-to-plate spacing can be seen in Figures 2 and 3. Analyses of the results are divided into three regions: Jet deflection region (Region I) ranging from 0.03<H/d<1.2; transition region (Region II) ranging from 1.2<H/d<3; and buoyancy effect region (Region III) ranging from 3<H/d<8.5. In the jet deflection region (Region I), as shown in Figures 2(a) and (b), 0.03<H/d<1.2, the Nusselt number decreases exponentially as the nozzle-to-plate spacing increases for both the free surface jet and the submerged jet due to the flow deflection of the impinging plate [5]. This trend corresponds to the trend of the stagnation pressure values from 0.03<H/d<1.2 as shown in Figures 3(a) and (b). The Nusselt number reaches a minimum value and remains constant as the nozzle exits the stagnation region and approaches the transition region (Region II). Here the jet has the highest stagnation pressure and velocity due to the exit area decrease which occurs the jet flow deflection. The higher pressure at low nozzle-to-plate spacing in Region I generates higher heat transfer performance [5, 9-12].

In Region II, 1.2<H/d<3, the stagnation Nusselt number and pressure of the free surface jets and submerged jets decrease with a gentle slope as it approaches Region III for all volumetric qualities since the stagnation pressure decreases by the decrease in jet deflection effect as the nozzle-to-plate spacing increases as shown in Figures 3(a) and (b).

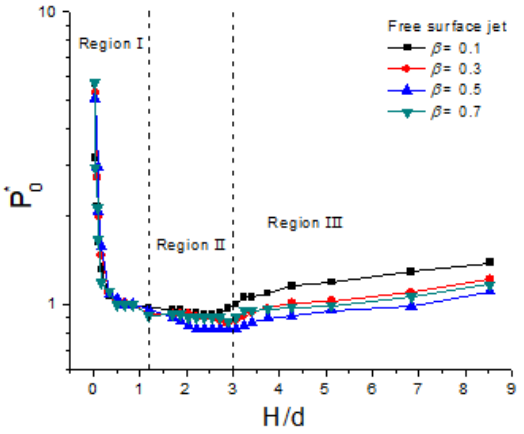


**Figure 2:** Normalized stagnation Nusselt number: (a) free surface jet (b) submerged jet.

In Region III, 3<H/d<8.5, the Nusselt number of the free surface jets for all volumetric qualities increases linearly as shown in Figure 2(a). This can be attributed to the increase in stagnation pressure by potential energy increase as the nozzle-to-plate spacing increase as shown in Figures 3(a) and 4(a). The longer water jet columns have higher potential energy and stagnation pressure in free surface jets at the higher nozzle-to-plate spacing. However, the Nusselt number and stagnation pressure of the submerged jets decreases linearly for all volumetric qualities as the nozzle-to-plate spacing is increased as shown in Figures 2(b) and 3(b). The bubbles have a larger distance to travel to reach the heated plate due to the buoyancy effect as shown in Figure 4(b). Because the jet is submerged, the jet must be forced through the water that separates it from the impingement surface.

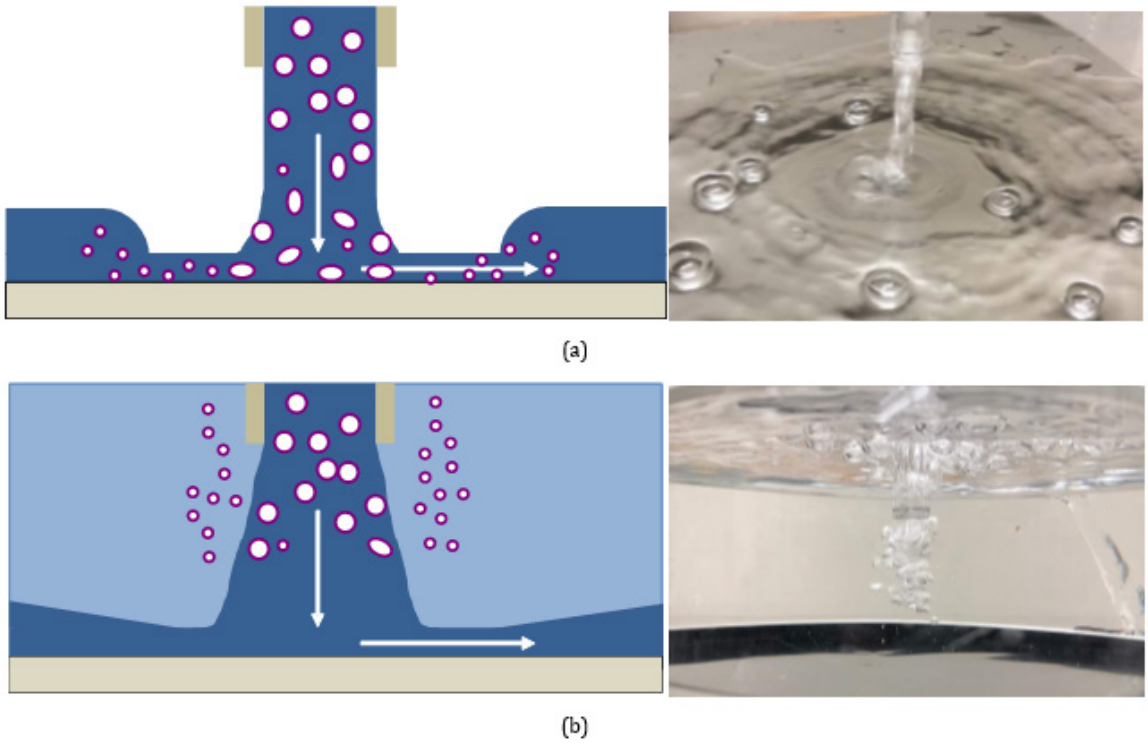


**Figure 4:** Flow visualization in Region III at H/d = 7: (a) free surface jet (b) submerged jet.

Comparing the values of the free surface and submerged jet, the free surface jet has a slightly higher Nusselt number for low nozzle-to-plate spacings as shown in Figure 5(a). As the nozzle-to-plate spacing increases, the Nusselt number of the submerged jet decreases while the Nusselt number of the free surface jet increases. At some point, they intersect and the free surface jet Nusselt number becomes larger than that of the submerged jet. The point of intersection varies for each volumetric quality, which occurs at H/d = 2 - 4. In Figure 5(a), the value of the submerged jet is only larger by a small amount until H/d=0.51 at β=0.1. From 2.05<H/d<3.24, the values are almost exactly the same, until the free surface jet increases and the submerged jet decreases. In Figure 5(b), the submerged jet Nusselt numbers are higher than the free surface jet up to the intersection due to the entrainment of the surrounding water at β=0.7. The impact of bubbles on the heating surface for the submerged jet decreases beyond the intersection points due to the buoyancy force, which is occurred by the surrounding water. The Nusselt number variation at volume trial quality of 0.3 and 0.5 showed similar patterns as the volumetric quality of 0.7. The diminishment of the bubble impact decreases the heat transfer performance of the submerged jet, while the jet column of the free surface jet has higher potential energy and generates higher heat transfer performance beyond the intersection point.

## Conclusion

In this work, an experimental study was conducted for a comparison of two-phase submerged jets and free surface jets. The Nusselt number and pressure decreased exponentially in both free surface and submerged jets for all volumetric qualities in Region I due to the jet deflection. The Nusselt number and pressure of the submerged jets and free surface jets continue to decrease since the jet deflection effect disappears in Region II. The Nusselt number and stagnation pressure increased in the free surface jet since the potential energy increases, while the Nusselt number and pressure decreased in the submerged jet since the bubbles are not impinged the plate due to the buoyancy effect in Region III. The submerged jet

showed higher heat transfer performance than the free surface jet up to the intersection points of H/d = 2 – 4 due to the entrainment of surrounding water, while the free surface jet had higher thermal performance than the submerged jet beyond the intersection points due to the diminishment of the bubble impact by buoyancy effect.

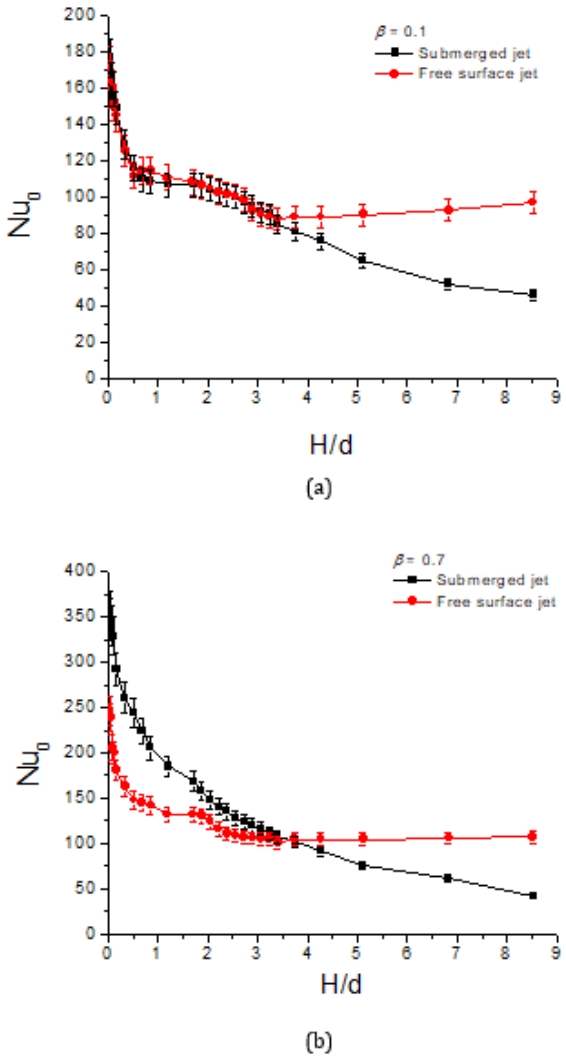


**Figure 5:** Comparison of Nusselt number between submerged and free surface jet.

## Acknowledgement

None.

## Conflict of Interest

There is no conflict of interest.

## References

1. Z Trávníček, V Tesař, Z Broučková, K Peszyński (2014) Annular Impinging Jet Controlled by Radial Synthetic Jets. Heat Transfer Engineering 35: 1450-1461.
2. A Dewan, R Dutta, B Srinivasan (2011) Recent Trends in Computation of Turbulent Jet Impingement Heat Transfer. Heat Transfer Engineering 33: 447-460.
3. C Agrawal, R Kumar, A Gupta, B Chatterjee (2016) Rewetting of Vertical Hot Surface during Round Water Jet Impingement Cooling. Heat Transfer Engineering 38: 1209-1221.
4. F Selimefendigil, H Öztop (2018) Al2O3-Water Nanofluid Jet Impingement Cooling With Magnetic Field. Heat Transfer Engineering 41(1): 50-64.
5. A Kuraan, SI Moldovan, K Choo (2017) Heat transfer and hydrodynamics of free water jet impingement at low nozzle-to-plate spacings. Int Journal of Heat and Mass Transfer 108: 2211-2216.
6. BK Friedrich, AW Glaspell, K Choo (2016) The Effect of Volumetric Quality on Heat Transfer and Fluid Flow Characteristics of Air-assistant Jet Impingement. Int Journal of Heat and Mass Transfer 101: 261-266.
7. K Choo, Friedrich BK, AW Glaspell, K Schilling (2016) The Influence of Nozzle-to-plate Spacing on Heat Transfer and Fluid Flow of Submerged Jet Impingement. International Journal of Heat and Mass Transfer 97: 66-69.
8. M Bieber, R Kneer, W Rohlfs (2017) Self-similarity of heat transfer characteristics in laminar submerged and free-surface slot jet impingement. International Journal of Heat and Mass Transfer 104: 1341-1352.

9. AW Glaspell, VJ Rouse, BK Friedrich, K Choo (2019) Heat transfer and hydrodynamics of air assisted free water jet impingement at low nozzle-to-surface distances. International Journal of Heat and Mass Transfer 132: 138-142.

10. BK Friedrich, TD Ford, AW Glaspell, K Choo (2017) Experimental study of the hydrodynamic and heat transfer of air-assistant circular water jet impinging a flat circular disk. International Journal of Heat and Mass Transfer 106: 804-809.

11. K Choo, SJ Kim (2016) The influence of nozzle diameter on the circular hydraulic jump of liquid jet impingement. Experimental Thermal and Fluid Science 72: 12-17.

12. K Choo, SJ Kim (2010) Heat transfer and fluid flow characteristics of two-phase impinging jets. International Journal of Heat and Mass Transfer 53: 5692-5699.